Journal of Wind Engineering & Industrial Aerodynamics 179 (2018) 308–318

Contents lists available at ScienceDirect

Journal of Wind Engineering & Industrial Aerodynamics

journal homepage: www.elsevier.com/locate/jweia

Numerical analysis of a vehicle wake with tapered rear extensions under yaw conditions

Magnus Urquhart [a,*], Simone Sebben [a], Lennert Sterken [b]

[a] Chalmers University of Technology, Sweden
[b] Volvo Car Corporation, Sweden

ARTICLE INFO

Keywords:
Tapered extensions
Yaw
Drag
Unsteady
Wake
POD

ABSTRACT

In recent years, governmental legislation and consumer demands are driving the development of more energy efficient road vehicles. One of the aspects considered when increasing efficiency is the aerodynamic performance of the vehicle. The focus of this paper is on wake effects for a vehicle with tapered rear extensions in side wind conditions. For this purpose, numerical simulations are analysed using post-processing techniques such as Proper Orthogonal Decomposition (POD) and Two-point correlation. The extensions protrude 150 mm from the perimeter of the base and are investigated in two configurations: with a smooth taper and with an added kick. The kick realigns the perimeter base flow to the vehicle's driving direction.

As the oncoming flow angularity is increased, drag increases for the investigated angles. The smooth extensions provide the greatest drag improvement at 0° yaw while the extensions with a kick yield additional benefits at yaw, effectively reducing the vehicles drag sensitivity to side wind. A large scale twisting motion is present at yaw for the baseline and smooth extensions configurations which is reduced when adding a kick to the extension.

1. Introduction

As part of the global efforts towards a sustainable society, OEMs are working on solutions to decrease emissions and increase the energy efficiency of road vehicles. Stricter emission targets, electric vehicle range and increased consumer demand are all driving factors in this development. The dominant source of resistance for a vehicle driving on a flat road at speeds above 80 km/h is the aerodynamic drag (Hucho, 1998). Reducing aerodynamic drag has become increasingly important with increasing road speeds and regenerative braking. This is reflected in the new standardised driving cycle WLTP which, compared to the previous driving cycle NEDC, puts more emphasis on the energy loss due to aerodynamic drag (Wittmeier et al., 2015).

Road vehicles are considered bluff bodies, and as such are characterised by massively separated wakes dominated by pressure drag. The pressure drag is largely dependent on the pressure difference between the front and rear end. To reduce the pressure difference, the rear end of road vehicles has been, and continues to be, an area of development and research. Different devices and methods have been tested to alter the wake flow and aid in the pressure recovery. Examples of such devices are: cavities, ventilated cavities, boat tailing flaps, passive bleed, short rear end tapers, vortex generators, synthetic jets, side skirts and blowing techniques (Duell and George, 1999; Jeff, 2012; Cooper, 2003; Irving Brown et al., 2010; Perry et al., 2016; Aider et al., 2010; Jonathan McNally et al., 2015; Kourta and Leclerc, 2013; Harinaldiet al, 2013; Bae Geun Hwang et al., 2016). The focus of this paper is on the wake flow features of a road vehicle with tapered rear end extensions, with and without an additional flow aligning feature referred to as a kick.

In a previous study, using the same vehicle geometry as in this investigation, Sebben et al. (2016) found a reduction in the unsteady surface pressure fluctuations when adding the extensions. Other authors have also reported a reduction in the unsteadiness of the wake using similar geometrical modifications (Duell and George, 1999; Khalighi et al., 2013). Perry (2016) investigated the wake characteristics on a simplified vehicle body for varying top and bottom tapers using particle image velocimetry. The lowest drag was found for a 16° top taper and a 6° bottom taper, yielding a balanced wake which impinged near half the base height. In the study several configurations were investigated and it was noted that the velocity magnitude within the wake was larger for the configuration with lowest drag compared to the baseline. Perry et al. (2016) investigated the wake closure point, size and the kinetic energy within the wake; however, no clear connection to drag was found.

This work further investigates the unsteady wake, for a vehicle with extensions, using velocity fields in three wake planes as well as unsteady

* Corresponding author.
E-mail address: magnus.urquhart@chalmers.se (M. Urquhart).

https://doi.org/10.1016/j.jweia.2018.06.001
Received 17 February 2018; Received in revised form 1 June 2018; Accepted 1 June 2018

surface pressure measurements from numerical simulations. The results are analysed in straight and yawed flow conditions using spectral methods and Proper Orthogonal Decomposition (POD). POD is a modal decomposition technique and has been used to investigate fluid flows and extract turbulent structures (Sebben et al., 2016; Tairaet al, 2017). The investigation is performed for three geometrical configurations: without extensions, referenced to as the baseline (*A*); with smooth tapered extensions (*B*) and tapered extensions with kick, (*C*). All three geometrical configurations are investigated in 0°, 2.5° and 5° yaw representing a continuous side wind condition.

2. Methodology

The geometry and the numerical procedure including post processing techniques are described in this section.

2.1. Geometry

The test object used in this study is a modified version of a Volvo XC60 AWD, which has been used in previous studies (Sebben et al., 2016; Sterkenet al, 2014; Sterkenet al, 2015). The full size, fully detailed geometry features additional underbody panels as shown in Fig. 1. The additional underbody panels were added to improve the flow quality from under the vehicle to the wake. The upper and lower grille are closed for all configurations.

The extensions are placed at the base and cover the top and sides of the vehicle, see Figs. 2 and 3. The taper is increased by approximately 5°, compared to the vehicles original taper of approximately 10°. The extensions are 150 mm long, where the last 50 mm of the extensions with a kick is aligned with the driving direction, as shown in Fig. 2. The configurations will hereon be called: baseline, *A*, smooth extensions, *B*, and extensions with a kick *C*.

2.2. Numerical set-up

The numerical simulations were performed using Star-CCM+, which is a Finite Volume Method (FVM) CFD solver. The turbulence is modelled using a hybrid RANS-LES, two equation Improved Delayed Detached Eddy Simulation (IDDES) SST k-ω turbulence model. A 2nd-order temporal and spatial discretization scheme is used where the gradients are computed using a hybrid Gauss-Least Squares method (Hybrid-LSQ). All simulations are run incompressible at 100 km/h. The resulting Reynolds number is approximately 3×10^6 based on the vehicle length.

The simulations were run on 2000 cores where each simulated physical second required approximately 16000 core hours. In total, with all simulations included, 81 physical seconds were run resulting in approximately 1.3×10^6 core hours. Simulations which have been run in order to investigate the simulation setup are not included in the 1.3×10^6 core hours.

The timestep used is $2.5 \times 10^{-4} s$, giving an average convective Courant number of 0.9, with more than 70% of the cells being below 1. The Courant number for a cell is defined as $C = |V|\Delta t/\sqrt[3]{C_V}$, where Δt and C_V is the timestep and cell volume respectively. The averaged velocity field is used to calculate the convective Courant number. However, accelerated flow and fluctuations around the car may cause the Courant number to be larger than 1 locally. The influence of the time step was investigated by reducing it to $1.0 \times 10^{-4} s$, showing less than $0.001 \Delta C_D$, or 0.3% difference in drag between the timesteps, where C_D is the non-dimensionalised drag force. C_D is defined as $C_D = F_D/0.5\rho V_\infty^2 A$ where V_∞ is the free-stream velocity and A is the vehicles projected frontal area. The average convective Courant number for the smaller time step was less than 0.4 with more than 90% of the cells being below 1. The number of inner iterations between timesteps is set to 7. The convergence within inner iterations was investigated in two points in the wake shear layer where the velocity was monitored. The flow reached convergence for the investigated points where the last 2–3 inner iterations showed little to no change in the monitored values.

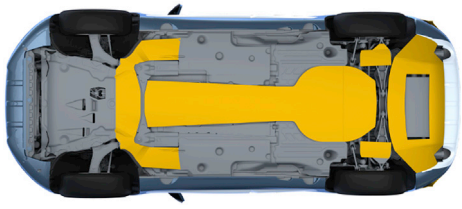

Fig. 1. Underbody with additional panels coloured in yellow. (For interpretation of the references to colour in this figure legend, the reader is referred to the Web version of this article.)

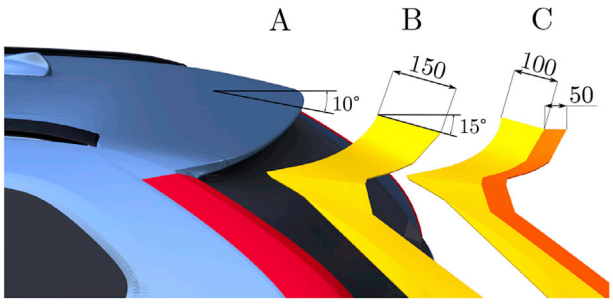

Fig. 2. Close-up of the extensions with measurements in [mm]. The taper angle is referenced to the horizontal plane.

Fig. 3. Rear view of the smooth extensions, configuration *B*.

Each case is comprised of approximately 130×10^6 hexahedral dominant cells where regions such as the wake shear layer, mirrors and underbody are refined. The majority of the car exterior and underbody panels, which are facing the external flow, have 12 prism layers spanning $8mm$ with a first cell height of $0.015mm$ resulting in a $y^+ < 1$ as required by the wall treatment. The resulting growth ratio in the near wall prism is 1.6 which, as investigated by Hobeika et al. (Hobeika and Sebben, 2018), was found to be adequate using a similar numerical setup, mesh resolution and Reynolds number. The wheel geometry is smooth and deformed to represent a loaded tire. The wheel rotation is modelled as a rotating wall with Moving Reference Frame (MRF) zones in the spokes, following the same setup as in (Sebben et al., 2016).

The mesh resolution in the separated wake region was evaluated using two-point correlation of the longitudinal velocities. According to Davidson (2009), the energy spectra, as well as the resolved turbulent kinetic energy ratio, are poor measures of LES resolution. A better alternative was found to be a two-point correlation, where the number of correlated cells gives an indication of the mesh resolution. The definition of two-point correlation is described in section 3.3.3.

A two-point correlation for twenty points was performed on the centerline plane for the baseline configuration without yaw. The mesh resolution of the centerline plane and three of the investigated locations can be seen in Fig. 4. The reference cell used for the correlation is the cell